https://doi.org/10.1016/j.jnoncrysol.2019.01.006
This is the Pre-Published Version.

On the variation of the mechanical energy accumulation rates during the flow serrations of a Zr-based bulk metallic glass

H.Y. Cheng[1], S.H. Chen[1,2]*, Y.Q. Qin[2,3], S.D. Feng[4], K.C. Chan[4], and Y.C. Wu[2,3]*

[1]School of Mechanical Engineering, Hefei University of Technology, Hefei 230009, China

[2]National-Local Joint Engineering Research Centre of Nonferrous Metals and Processing Technology, Hefei 230009, China

[3]School of Materials Science and Engineering, Hefei University of Technology, Hefei 230009, China

[4]Advanced Manufacturing Technology Research Centre, Department of Industrial and Systems Engineering, The Hong Kong Polytechnic University, Hung Hom, Kowloon, Hong Kong

* Corresponding author. shchen@hfut.edu.cn (S.H. Chen) & ycwu@hfut.edu.cn (Y.C. Wu)

Abstract

Bulk metallic glasses (BMGs) have serrated flows to accommodate plastic deformation at room temperature, where the mechanical energy is accumulated in a stress arising process and then released by a following stress drop. In this study, the variation of the mechanical energy accumulation rate of a Zr-based BMG under varying external disturbances, including the geometric confinement, sample sizes and stress gradients, has been investigated at varying strain rates. In all groups of specimens, the accumulation rates for the elastic strain energy during the plastic-flow serrations are different from the values at the initial elastic stages under compression tests, and have large variations. The variations of the accumulation rates are affected by the applied strain rates, and smaller variations are observed at relatively-lower strain rates (5×10^{-4} s^{-1} and 5×10^{-5} s^{-1}). Such variations in the change of the applied strain rates are independent of the presence of the geometric confinement, size effect and stress gradients, and may be attributed to the intrinsic deformation mechanisms of BMGs. The findings give further insights into the mechanisms on the evolution of

flow serrations in BMGs.

Key words: Bulk metallic glass; Statistical analysis; Serration; Mechanical energy.

1. Introduction

Bulk metallic glasses (BMGs) form a class of amorphous alloys with unusual mechanical properties, such as high strength and large elastic limit that are superior to the conventional crystalline alloys, and have great potential for practical structural applications [1-7]. Understanding of the room-temperature plastic deformation mechanisms of BMGs plays a key role in achieving their widespread applications as structural materials. At room temperature, the plastic deformation of BMGs is highly localized in thin layers of shear bands, demonstrating serrated plastic flows in the stress-strain curves [8, 9]. The formation of the serrations is significantly affected by the applied strain rates [10-12] and external disturbances, such as the geometric confinement [9, 13] and stress gradients [14-16]. For example, Schuh et al. showed that with increasing loading rates, the plastic deformation in BMGs transits from serrated flows into homogeneous deformation [11]. Introducing appropriate stress fields can drive bursts of more plastic flows which can evolve to a critical dynamics and lead to the delay of catastrophic failure [15]. During the plastic-flow stage of BMGs, the strain energy is firstly accumulated and stored, leading to a stress arising, which is usually considered as an elastic energy accumulation process [9]. When the amount of accumulated elastic energy reaches a critical value, the energy is released by the formation and propagation of a shear band, resulting in a stress drop [8]. Since the mechanisms on the initiation and propagation of shear bands are still being debated [17], studies on the serrations may be helpful in uncovering the corresponding plastic deformation mechanisms. For instance, what is the difference between the elastic strain energy accumulation process during the flow serration stage and at the initial elastic stage?

With stochastic atomic orders, the mechanical properties of BMGs, such as strength

[18-20], plasticity [21] and fracture toughness [22,23], demonstrate variations from specimen to specimen. Similarly, the flow serrations in BMGs also demonstrate large variations, for example, the magnitudes and elastic strain energy accumulation rates (ESEARs). The evolution of the magnitudes of the serrations has been examined extensively using statistical analysis, where some data follow a power-law and can evolve to a critical state [9,15,24,25]. However, studies focused on the variation of the ESEAR values, which is associated with the capacity of the BMG to accommodate the elastic strain energy during the plastic deformation processes, have rarely been reported. The change of the ESEAR affects the capability of BMGs to accommodate the plastic deformation energy. In a recent work, Tang et al. [26] reported the achievement of a relatively high uniformity of ESEAR under a constrained complex stress field. It suggests that the evolution of ESEAR is significantly dependent on the confinement of the propagation of shear bands. Consequently, how about the variation of ESEARs under varying external disturbances, where BMGs have improved macroscopic plasticity? The BMG specimens used in Ref. [26] deformed under a mixed-mode loading condition, where investigation of ESEARs under standard tests may give more insight into the mechanisms on the evolution of ESEAR during the serration flows. In this work, the variation of ESEARs in a Zr-based BMG has been examined under compression tests at varying strain rates. The effect of external disturbances, such as the geometric confinement, sample sizes and stress gradient, on the variation of ESEARs has also been investigated. The results have shown that the variations of the ESEARs may be intrinsic for BMGs, which are independent on the applied external disturbances, such as geometric confinement, sample sizes and gradient stress distributions.

2. Experimental

Cylindrical as-cast BMG rods ($Zr_{57}Cu_{20}Al_{10}Ni_8Ti_5$, *at*.%) were fabricated by suction casting using a water-cooled copper mold. Four groups of specimens were employed to obtain serrated plastic flows under varying external disturbances: Group I, BMG specimens of 2 mm diameter; Group II, geometric confined BMG specimens with 2

mm in diameter, where a Ni layer with thickness of 66 ± 7 μm was electroplated onto the side surface; Group III, BMG specimens of 3 mm diameter; and Group IV, BMG specimens of 3 mm diameter with a tilted angle of 2 degree on the top surface, which can result in the presence of stress gradients during the compressive tests [13]. The room-temperature compression testing of the specimens with an aspect ratio of 2 were conducted on an MTS Qtest/25 materials testing machine at strain rates of 5×10^{-3} s^{-1}, 5×10^{-4} s^{-1} and 5×10^{-5} s^{-1}, respectively. The data for the serrated plastic flows were collected at a rate of 50 data per second. To investigate the variation of the mechanical energy accumulation rates, the Weibull distribution was employed, which has been widely used to evaluate the variation of the strength and plasticity of BMGs [18-21,27].

3. Results and discussion

Fig. 1a shows the representative stress-time curves of group I specimens (the stress-time curves of groups II-IV specimens are given in Fig. SI1 in the Supplementary Materials). It can be seen that, after the elastic stage, the specimens showed serrated plastic-flow stages at different strain rates. The typical serrated flows of the specimen at a higher magnification are given in Fig. 1b. With the decrease of strain rate, more serrations were obtained. The number of serrations against the decreasing strain rates is plotted in Fig. 2. It can be seen that, for all groups of specimens, decreasing of the strain rate can trigger the burst of more serrations. The dynamics of the flow serrations in BMGs can be classified into two states: one is chaotic dynamics, and the other is a power-law criticality behavior (or a self-organized critical state, i.e., an SOC behavior) [9,15,24]. The criticality of the plastic flows depends on the geometric confinement, sample sizes and complex stress fields [9,13,15]. However, the determining of the dynamics of flow serrations depends significantly on the amplitudes/sizes of the stress/load drops. The present work aims to characterize the flow serrations based on the ESEARs, i.e., during the stress-arising process, which may give more insight into the deformation mechanisms of BMGs. To compare the ESEARs of different serrations, we define the accumulation rate of a

single serration at the plastic-flow stages as $E_p = \delta_\sigma/\delta_t$ (Fig. 1b). For the initial elastic stage, the ESEAR is denoted as E_e. In the magnified stress-time curves (Fig. 1b), it can be seen that there is an obvious variation of the E_p values.

The E_p values of the four groups of specimens were collected, as shown in Fig. 3. All specimens showed large variations in ESEAR values, regardless of the applied strain rates and the external disturbances (the geometric confinement, sample sizes and stress gradients). For example, the group I specimen at a strain rate of 5×10^{-3} s^{-1} had the smallest value of 16.7 MPa/s, and the largest value (170.5 MPa/s), about ten times of the smallest one. Although previous research has shown that the presence of external disturbances can reduce the variation of the plasticity on the change of strain rates or samples [13], they have limited effect on the variations of the E_p values. The large variations suggest that during the plastic-flow stage, the burst of each serration cannot be considered as an independent elastic event similar to the elastic stages of the specimen, and the burst of each serration should be dependent on the formation of previous serrations. The plastic-flow dynamics of the two-stage serrated flows have also shown that the triggering of the burst of serrations was affected by the previous ones [15]. Therefore, a statistical analysis should be helpful in understanding the mechanisms of the flow serrations.

The detailed statistical results of the E_p values of the plastic-flow serrations are given in Table 1. Overall, with the decreasing of strain rate, a larger time range (δ_t) will be achieved, resulting in smaller E_p values. However, as compared with the accumulation rates at the elastic stage (E_e), the average values for the serrations (E_a) demonstrate differences on the change of strain rates. At a relatively-high strain rate of 5×10^{-3} s^{-1}, the E_a value is smaller than the E_e value. While at relatively-low strain rates of 5×10^{-4} s^{-1} and 5×10^{-5} s^{-1}, the E_a values are larger than the E_e values. Such a trend is independent on the applied external disturbances (geometric confinement, size effect and stress gradient). It can be concluded that despite the variations, a relatively-higher strain rate tends to result in a decrease of ESEAR. When the applied strain rate

increases beyond a critical value, the elastic energy accumulation process could be eliminated, resulting in a non-serrated flow. In fact, such predictions are highly in line with the molecular dynamics (MD) simulation results on the plastic deformation of MGs at high strain rates up to 1×10^{8} s^{-1}, where serrated plastic flows were not observed [28,29]. The transition from serrated to non-serrated plastic flows has also been evidenced by the nanoindentation tests of BMGs [11,30]. A lower loading rate can promote the formation of more serrations while a higher loading rate tends to suppress the formation of the serrated flows. To better compare the differences of the accumulation rates between the elastic and serrated-plastic-flow stages, the ratio, E_a/E_e, was plotted against the strain rates, as shown in Fig. 4. It can be seen that the E_a/E_e ratio increases with decreasing applied strain rate. This implies that even at relatively lower strain rates, the ESEAR during the plastic-flow stages is also sensitive to the applied strain rates.

In order to assess the variation of the ESEARs during the serrated plastic flows, the data in Fig. 3 were fitted using a three-parameter Weibull distribution. The Weibull distribution has been used extensively to assess the reliability of materials in engineering applications, and has also been used to evaluate the variation of the strength of brittle materials, including BMGs [18,19,27,31]. The cumulative distribution of the accumulation rates is given as

$$P_e = 1 - \exp\left[-\left(\frac{E - E_\mu}{E_0}\right)^m\right] \quad (1)$$

where P_e is the probability for a given ESEAR value E, E_0 is a scaling parameter, m is the Weibull modulus, and E_μ is a cut-off value. The fitting parameters can then be obtained by linearizing the equation (1), as shown in the following equation:

$$\ln\left[\ln\left(\frac{1}{1-P_e}\right)\right] = m\ln(E - E_\mu) - m\ln(E_0) \quad (2)$$

The modulus of the Weibull distribution, m, reflects the scattering of the data. The probability plots of the specimens are shown in Fig. 5 and Fig. SI2-4 in the Supplementary Materials, respectively. The fitting data are also listed in Table 1 (due to the limited number of serrations smaller than 20, the fitting results of the elastic

strain energy accumulation rates of the group III specimens at strain rates of 5×10^{-3} s^{-1} and 5×10^{-4} s^{-1} are only listed for reference [21,27]). According to the fitting results, the moduli of the ESEARs of the plastic flow serrations are much smaller than the distribution of the strength (for example, 5.98-6.80 in Ref. [18], 11-45.7 in Ref. [19], and 36.5 in Ref. [20]), but larger than the plasticity of the BMG specimens (0.92-1.92 in Ref. [21]). A smaller modulus means that the data are less concentrated, and have relatively larger variations.

Look into the fitting results in detail, for each group of the specimens, the Weibull modulus has the smallest value at a relatively-higher strain rate of 5×10^{-3} s^{-1}. At the relatively-lower strain rates of 5×10^{-4} s^{-1} and 5×10^{-5} s^{-1}, the modulus increases, suggesting smaller variations. As compared with the Weibull modulus at the lowest strain rate of 5×10^{-5} s^{-1}, the Weibull modulus of the medium strain rate (5×10^{-4} s^{-1}) has the largest value, indicating the smallest variation. The findings imply that the variation of ESEAR is dependent on the applied strain rates. Based on the assumption that the BMGs have the same elastic responses at the initial elastic stage at varying strain rates, the E_e values should also be proportional to the applied strain rates. By defining the E_e values at strain rates of 5×10^{-3} s^{-1}, 5×10^{-4} s^{-1}, and 5×10^{-5} s^{-1} as E_{e1}, E_{e2} and E_{e3} respectively, there should be a relationship as $E_{e1} = 10E_{e2} = 100E_{e3}$. As compared with the E_e values in Table 1, we found that between the strain rates 5×10^{-3} s^{-1} and 5×10^{-4} s^{-1}, all groups of specimens have the relationships $E_{e1} \approx 10E_{e2}$. This suggests that the BMG specimens do not show significant differences on the change of the strain rate from 5×10^{-3} s^{-1} to 5×10^{-4} s^{-1} at the initial elastic stage, where the decrease of the Weibull modulus is mainly attributable to the different responses of the BMGs during the plastic deformation stages due to the change of the strain rates. However, when the strain rate changes from 5×10^{-4} s^{-1} to 5×10^{-5} s^{-1}, the relationship changes to $E_{e2} = (3.82\text{-}4.48)E_{e3}$. This implies that at the initial elastic stage, the BMG already has different responses to the change of the strain rate, which may also affect the variation of ESEARs during the serrated-plastic flow stages. This might be the reason why all groups of specimens have relatively-smaller Weibull moduli at a strain

rate of 5×10^{-5} s^{-1} (Table 1). Although more effort is needed to uncover the mechanisms of the effect of strain rates on the change of the Weibull modulus, it can be concluded that at relatively-low strain rates (5×10^{-4} and 5×10^{-5} s^{-1}), the ESEAR has smaller variations during the serrated plastic-flow stages.

The high repeatability of the strength of BMGs is better than that of some other brittle solids, such as the ceramics. The small variation of the strength of BMGs may result from the high flaw tolerance of BMGs, where the specimens with minor casting defects are not sensitive to the cracks [20]. The plasticity of BMGs is significantly dependent on the intrinsic variability of the atomic arrangements inherited from the solidification processes [21]. It can be concluded that both the variations of the strength and plasticity are mainly caused by the variation of the atomic structures stemming from the fabrication processes. However, the ESEAR at the initial elastic stage of deformation, i.e., the E_e value, is associated with the yield strength of BMGs, which also has small variation [32]. The change of the E_a/E_e ratios (Fig. 4) shows that the ESEARs of the flow serrations (E_p) are different from the E_e values. During the plastic-flow stages, some shear bands are formed, resulting in a work-softening-like effect, where the atomic structures of BMGs are also changed. The accumulation of the elastic strain energy is then influenced by the deformed parts of the specimen, resulting in a different accumulation rate from the initial elastic stage. Since the bursts of the serrations are associated with the formation of shear bands [8] and the serrated flows are also related to the multiplication and intersection of shear bands [33], the accumulation of the elastic strain energy of the serrations should be affected by previous existing serrations. The variations of the E_p values can then be understood as that the formation, propagation and intersection of the shear bands of BMGs are spatially and temporally different during the loading process. Nevertheless, the change of the Weibull moduli of the variations of the E_p values on the change of the applied strain rates suggests that there may exist some relationships among the ESEARs of the flow serrations, similar to the criticality behavior, based on the statistics of the magnitudes [9,15,24,25]. The authors would like to point out that the

Many studies have shown that BMGs can demonstrate different deformation behavior under varying external disturbances. Wide plastic-flow-plateau stages can be obtained by reducing the sample sizes [34-36], introducing geometric confinement [37,38] and tailoring complex stress distributions [39-41]. The nominal plasticity of BMGs has shown less dependence on the strain rates with the presence of some external disturbances, such as the geometric confinement and stress gradients [13]. The presence of stress gradients can also result in small variations in the nominal plasticity [21]. However, the present work has shown that the large variations of the ESEARs occur in all groups of specimens, and shown similar trends on the change of the strain rates. The variation of ESEAR during the flow serrations may result from the intrinsic deformation mechanisms of the BMGs. This further confirms that some underlying laws may exist among the serrations, similar to the power-law criticality behavior [9,15,24,25]. Understanding the intrinsic variations of the mechanical accumulation rates in BMGs could be helpful for uncovering the mechanism of the bursts of serrated plastic flows. For example, it is challenging for the present constitutive models of BMGs to capture the serrated flows of BMGs [42-45]. The uncovering of the intrinsic connections of ESEARs during the flow serrations may be helpful for building an intrinsic relationship between the loading and plastic deformation of BMGs. The present work has shown the intrinsic variations of ESEARs and revealed their dependence on the change of the strain rates. However, more effort is still necessary to shed more light into the intrinsic connections of the serrations, for example, how the triggering of the burst of a serration is affected by the previous existing serrations?

4. Conclusions

In summary, the variation of ESEARs of the flow serrations in BMGs under external disturbances, such as geometric confinement, sample sizes and stress gradient, has been studied under varying strain rates. The main findings are concluded as:

- Large variations of ESEARs during the flow serrations, which are different from

the ESEARs at the initial elastic stage, have been observed, demonstrating differences on the change of applied strain rates.

- At a relatively-high strain rate of 5×10^{-3} s^{-1}, the specimens have relatively smaller Weibull moduli, which are associated with larger variations in ESEARs. While at relatively-low strain rates (5×10^{-4} and 5×10^{-5} s^{-1}), all groups of specimens have larger Weibull molduli, suggesting smaller variations.
- The large variations in ESEARs as well as the trends on the change of the applied strain rates are similar for all groups of specimens, regardless of the presence of external disturbances, such as the geometric confinement, sample sizes and stress gradients. The large variations of ESEARs in flow serrations may result from the intrinsic deformation mechanisms of BMGs.

Acknowledgements

The work described in this paper was fully supported by a grant from the National Natural Science Foundation of China under research project No. 51801049.

References

[1] J. Plummer, W.L. Johnson, Nat. Mater., 14 (2015) 553-555.

[2] S.H. Chen, K.C. Chan, F.F. Wu, L. Xia, Appl. Phys. Lett., 104 (2014) 111907.

[3] Y.C. Lin, Y.C. Tsai, T. Ono, P. Liu, M. Esashi, T. Gessner, M.W. Chen, Adv. Funct. Mater., 25 (2015) 5677-5682.

[4] D.C. Hofmann, L.M. Andersen, J. Kolodziejska, S.N. Roberts, J.P. Borgonia, W.L. Johnson, K.S. Vecchio, A. Kennett, Adv. Eng. Mater., (2016) 1600541.

[5] S.H. Chen, K.C. Chan, T.M. Yue, F.F. Wu, Scripta Mater., 142 (2018) 83-87.

[6] H.J. Xian, C.R. Cao, J.A. Shi, X.S. Zhu, Y.C. Hu, Y.F. Huang, S. Meng, L. Gu, Y.H. Liu, H.Y. Bai, W.H. Wang, Appl. Phys. Lett., 111 (2017) 121906.

[7] M.M. Trexler, N.N. Thadhani, Prog. Mater. Sci., 55 (2010) 759-839.

[8] S.X. Song, H. Bei, J. Wadsworth, T.G. Nieh, Intermetallics, 16 (2008) 813-818.

[9] G. Wang, K.C. Chan, L. Xia, P. Yu, J. Shen, W.H. Wang, Acta Mater., 57 (2009) 6146-6155.

[10] T.C. Hufnagel, T. Jiao, Y. Li, L.Q. Xing, K.T. Ramesh, J. Mater. Res., 17 (2002) 1441-1445.

[11] C.A. Schuh, A.S. Argon, T.G. Nieh, J. Wadsworth, Philos. Mag., 83 (2003) 2585-2597.

[12] J. Hu, B.A. Sun, Y. Yang, C.T. Liu, S. Pauly, Y.X. Weng, J. Eckert, Intermetallics, 66 (2015) 31-39.

[13] S.H. Chen, T.M. Yue, C.P. Tsui, K.C. Chan, Mater. Sci. Eng. A, 669 (2016) 103-109.

[14] R.T. Qu, J.X. Zhao, M. Stoica, J. Eckert, Z.F. Zhang, Mater. Sci. Eng. A, 534 (2012) 365-373.

[15] S.H. Chen, K.C. Chan, G. Wang, F.F. Wu, L. Xia, J.L. Ren, J. Li, K.A. Dahmen, P.K. Liaw, Sci. Rep., 6 (2016) 21967.

[16] S.H. Chen, T.M. Yue, C.P. Tsui, K.C. Chan, Sci. Rep., 6 (2016) 36130.

[17] A.L. Greer, Y.Q. Cheng, E. Ma, Mater. Sci. Eng. R, 74 (2013) 71-132.

[18] Z. Han, L.C. Tang, J. Xu, Y. Li, Scripta Mater., 61 (2009) 923-926.

[19] C.J. Lee, Y.H. Lai, J.C. Huang, X.H. Du, L. Wang, T.G. Nieh, Scripta Mater., 63 (2010) 105-108.

[20] L. Lu, J.H. Yao, J.Q. Wang, Y. Li, Appl. Phys. Lett., 92 (2008) 041905.

[21] J.J. Fan, Y.F. Yan, S.H. Chen, C.H. Ng, F.F. Wu, K.C. Chan, Intermetallics, 74 (2016) 25-30.

[22] R.L. Narayan, P. Tandaiya, G.R. Garrett, M.D. Demetriou, U. Ramamurty, Scripta Mater., 102 (2015) 75-78.

[23] W. Chen, J. Ketkaew, Z. Liu, R.M.O. Mota, K. O'Brien, C.S. da Silva, J. Schroers, Scripta Mater., 107 (2015) 1-4.

[24] B.A. Sun, H.B. Yu, W. Jiao, H.Y. Bai, D.Q. Zhao, W.H. Wang, Phys. Rev. Lett., 105 (2010) 035501.

[25] J.J. Li, Z. Wang, J.W. Qiao, Mater. Design., 99 (2016) 427-432.

[26] H.H. Tang, Y.C. Cai, Q. Zou, S.H. Chen, R.P. Liu, Mater. Sci. Eng. A, 736 (2018) 269-275.

[27] P. Jia, Z.D. Zhu, X.W. Zuo, E.G. Wang, J.C. He, Intermetallics, 19 (2011)

1902-1907.

[28] A.J. Cao, Y.Q. Cheng, E. Ma, Acta Mater., 57(2009) 5146-5155.

[29] S. D. Feng, L.M Wang, S.P. Pan, M.Z. Ma, X.Y. Zhang, G. Li, R.P. Liu, Acta Mater., 95(2015) 236-243.

[30] C.A. Schuh, T.G. Nieh, Acta Mater., 51 (2003) 87-99.

[31] W.F. Wu, Y. Li, C.A. Schuh, Philos. Mag., 88 (2008) 71-89.

[32] W.H. Wang, Prog. Mater. Sci., 57 (2012) 487-656.

[33] B.A. Sun, S. Pauly, J. Tan, M. Stoica, W.H. Wang, U. Kuhn, J. Eckert, Acta Mater., 60 (2012) 4160-4171.

[34] N. Li, Q. Chen, L. Liu, J. Alloys Compd., 493 (2010) 142-147.

[35] Y.J. Huang, J. Shen, J.F. Sun, Appl. Phys. Lett., 90 (2007) 081919.

[36] F.F. Wu, Z.F. Zhang, S.X. Mao, J. Eckert, Phil. Mag. Lett., 89 (2009) 178-184.

[37] W. Chen, K.C. Chan, S.F. Guo, P. Yu, Mater. Lett., 65 (2011) 1172-1175.

[38] W. Chen, K.C. Chan, S.H. Chen, S.F. Guo, W.H. Li, G. Wang, Mater. Sci. Eng. A, 552 (2012) 199-203.

[39] W.F. Wu, C.Y. Zhang, Y.W. Zhang, K.Y. Zeng, Y. Li, Intermetallics, 16 (2008) 1190-1198.

[40] S.H. Chen, K.C. Chan, L. Xia, Mater. Sci. Eng. A, 574 (2013) 262-265.

[41] S.H. Chen, K.C. Chan, L. Xia, Intermetallics, 43 (2013) 38-44.

[42] Z. Lu, W. Jiao, W.H. Wang, H.Y. Bai, Phys. Rev. Lett., 113 (2014) 045501.

[43] L. Anand, C. Su, J. Mech. Phys. Solids, 53 (2005) 1362-1396.

[44] F. Spaepen, Scripta Mater., 54 (2006) 363-367.

[45] Y.F. Gao, Modell. Simul. Mater. Sci. Eng., 14 (2006) 1329-1345.

Figure captions

Fig. 1. (a) The nominal stress-time curves of the group I specimens at strain rates of 5 × 10^{-3}, 5 × 10^{-4} and 5 × 10^{-5} s^{-1}, respectively. (b) Magnified curve of the specimen at the strain rate of 5 × 10^{-4} s^{-1}, where the variation of ESEARs for different serrations (E_p) can be observed.

Fig. 2. The number of serrations of four groups of specimens collected at varying strain rates.

Fig. 3. The distribution of ESEARs of the flow serrations, where the collected data are plotted as the increase of the magnitude.

Fig. 4. The distribution of E_a/E_e ratios on the change of applied strain rates.

Fig. 5. The Weibull distribution showing the fitting results of ESEAR for group I specimens.

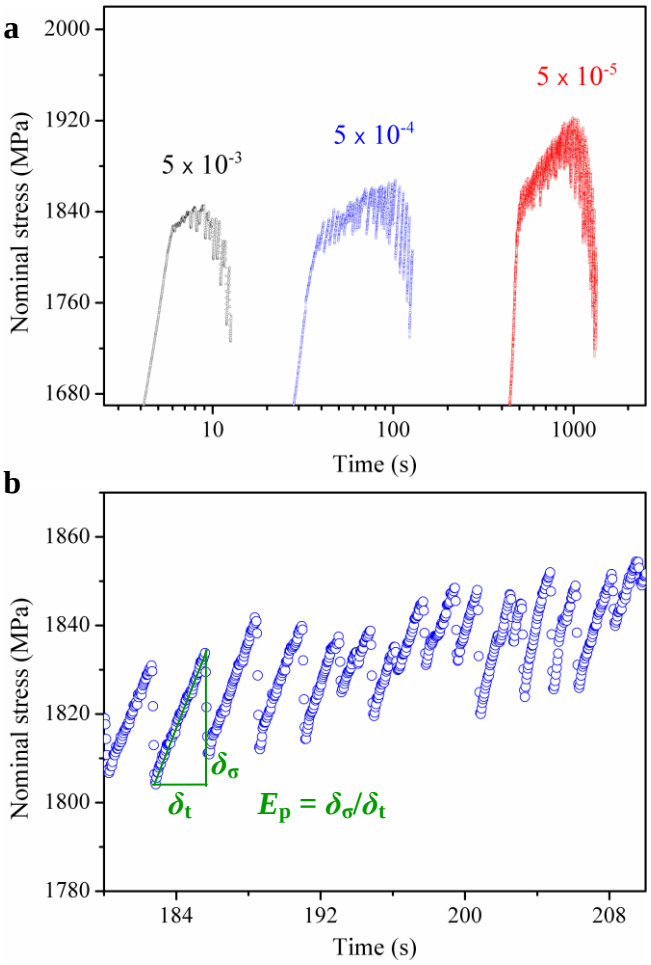

H. Y. Cheng *et al*.

Figure 1

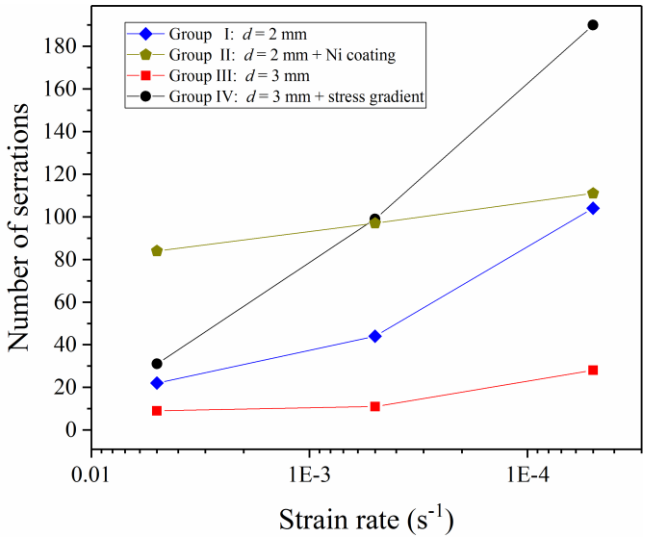

H. Y. Cheng *et al*.

Figure 2

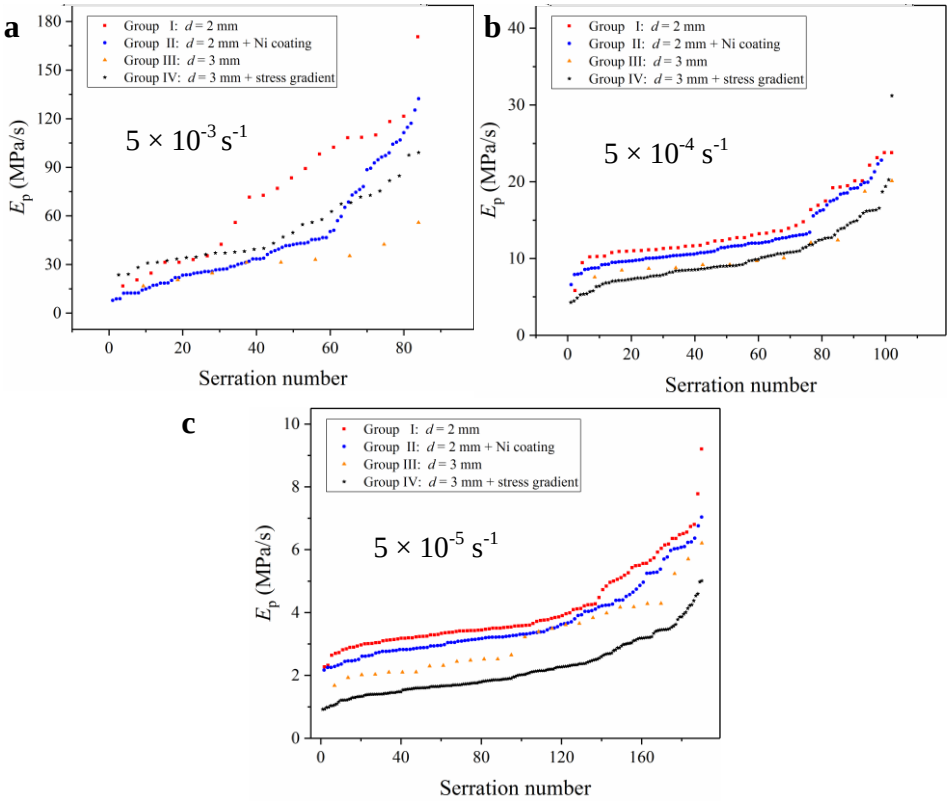

H. Y. Cheng *et al*.

Figure 3

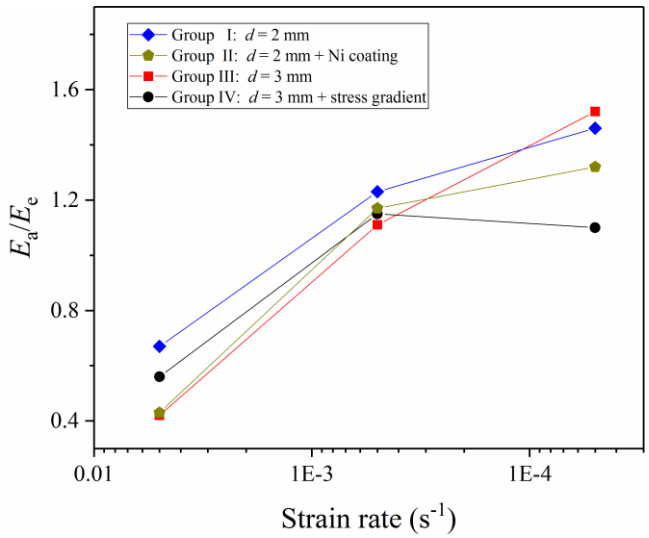

H. Y. Cheng *et al*.

Figure 4

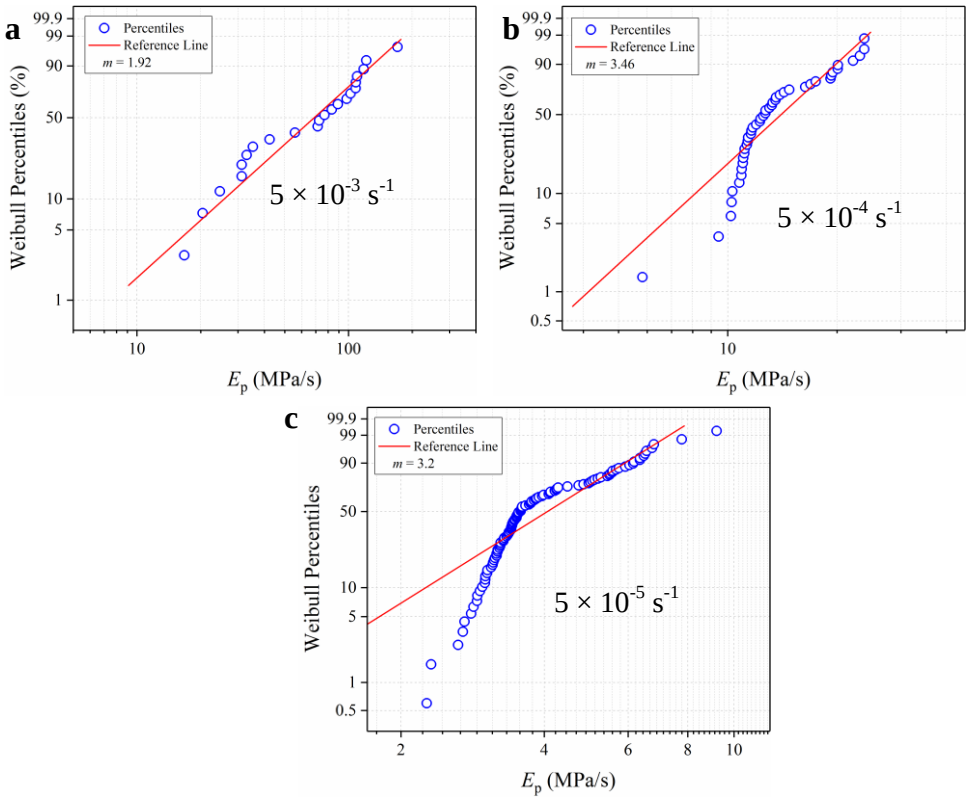

H. Y. Cheng *et al*.

Figure 5

Table 1. The statistical results of the E_p values of four groups of specimens, where N is the number of the serrations, E_a and E_s are the average value and standard deviation, respectively, and m is the three-parameter Weibull modulus.

Group	Strain rate (s^{-1})	E_e (MPa/s)	N	E_a (MPa/s)	E_s (MPa/s)	Minimum E_p (MPa/s)	Maximum E_p (MPa/s)	m
I	5×10^{-3}	110.7	22	73.7	41.2	16.7	170.5	1.92
I	5×10^{-4}	11.4	44	14.0	4.3	5.8	23.8	3.46
I	5×10^{-5}	2.8	104	4.1	1.3	2.3	9.2	3.2
II	5×10^{-3}	106.4	84	46.2	32.2	7.9	132.3	1.55
II	5×10^{-4}	10.7	97	12.5	3.7	6.6	22.8	3.5
II	5×10^{-5}	2.8	111	3.7	1.2	2.2	7.0	3.3
III	5×10^{-3}	95.1	9	40.2	18.9	21.8	82.5	2.38
III	5×10^{-4}	9.4	11	10.4	3.1	7.6	18.7	3.37
III	5×10^{-5}	2.1	28	3.2	1.2	1.7	6.2	2.89
IV	5×10^{-3}	88.8	31	49.9	20.9	23.7	99.1	2.59
IV	5×10^{-4}	8.8	99	10.1	3.3	4.9	20.3	3.19
IV	5×10^{-5}	2.0	190	2.2	0.9	0.9	5.0	2.68